Progress in Scale Modeling, an International Journal

Volume 3 | Issue 1 Article 4

2022

Scale modeling of an appearance of downwash pattern of hot smoke ejected from chimney in the turbulent cross flow

Xangpheuak Inthavideth
Toyohashi University of Technology, xangpheuak.inthavideth.pj@tut.jp

Nobumasa Sekishita
Toyohashi University of Technology, seki@me.tut.ac.jp

Sounthisack Phommachanh
National University of Laos, sounthisack@fe-nuol.edu.la

Yuji Nakamura
Toyohashi University of Technology, yuji@me.tut.ac.jp

Recommended Citation

Inthavideth, Xangpheuak; Sekishita, Nobumasa; Phommachanh, Sounthisack; and Nakamura, Yuji (2022) "Scale modeling of an appearance of downwash pattern of hot smoke ejected from chimney in the turbulent cross flow," *Progress in Scale Modeling, an International Journal*: Vol. 3: Iss. 1, Article 4.
DOI: https://doi.org/10.13023/psmij.2022.03-01-04
Available at: https://uknowledge.uky.edu/psmij/vol3/iss1/4

Scale modeling of an appearance of downwash pattern of hot smoke ejected from chimney in the turbulent cross flow

Category

Research Article

Abstract

This study aims to elucidate the scaling law to provide the critical condition on appearance of the downwash pattern of the hot smoke ejected from a chimney in a turbulent cross flow. A specially designed wind tunnel with an active turbulence generator developed by Makita was adopted to offer a quasi-isotropic turbulence field in a lab-scale test facility. A heated jet with smoke is issued into the cross flow from the vertically oriented chimney placed in the test section of the wind tunnel. In this study, the experimental parameters considered are temperature of the heated jet (smoke), jet ejected velocity, and cross-wind velocity, respectively. In the previous work, only two-patterns were observed under the condition studied in quasi-isotropic turbulence condition, such as meandering motion in downstream (Mode V) and downwash (Mode VI). The boundary of these two modes is found to be sensitive to all three parameters, suggesting that all are similarly important to determine the boundary. The observed data are summarized in the physical plane of Reynolds number and modified jet-Froude number, and it was found that all plots are collapsed into the single line. This result suggests that the viscous effect around the chimney plays a role on the appearance of downwash pattern of the hot smoke. It is necessary to check whether the scaling law would work even though the larger scale is imposed, whose Reynolds number based on the chimney scale is large enough and viscous force becomes less important.

Keywords

Smoke plume, Chimney, Cross-flow, Downwash, Turbulence

Cover Page Footnote

This is a fully-reviewed paper expanded from work that was presented at the 9th International Symposium on Scale Modeling (ISSM9), held in March 2022 in Naples, Italy.

Progress in Scale Modeling, an International Journal, Vol. 3, Issue 1 (2022) Article 03-01-04, pp. 1–10
https://doi.org/10.13023/psmij.2022.03-01-04

Scale modeling of an appearance of downwash pattern of hot smoke ejected from chimney in the turbulent cross flow

X. Inthavideth [1, 2], N. Sekishita [1], S. Phommachanh [2], Y. Nakamura [1, *]

[1] *Department of Mechanical Engineering, Toyohashi University of Technology, 1-1 Hibarigaoka, Tempaku, Toyohashi 441-8580, Japan*

[2] *Department of Mechanical Engineering, National University of Laos, Lao-Thai friendship Rd., Si-sattanak District, Vientiane Capital, Box. 3166, Lao PDR*

E-mail: yuji@me.tut.ac.jp

Received June 5, 2022, Accepted September 24, 2022

Abstract

This study aims to elucidate the scaling law to provide the critical condition on appearance of the downwash pattern of the hot smoke ejected from a chimney in a turbulent cross flow. A specially designed wind tunnel with an active turbulence generator developed by Makita was adopted to offer a quasi-isotropic turbulence field in a lab-scale test facility. A heated jet with smoke is issued into the cross flow from the vertically oriented chimney placed in the test section of the wind tunnel. In this study, the experimental parameters considered are temperature of the heated jet (smoke), jet ejected velocity, and cross-wind velocity, respectively. In the previous work, only two-patterns were observed under the condition studied in quasi-isotropic turbulence condition, such as meandering motion in downstream (Mode V) and downwash (Mode VI). The boundary of these two modes is found to be sensitive to all three parameters, suggesting that all are similarly important to determine the boundary. The observed data are summarized in the physical plane of Reynolds number and modified jet-Froude number, and it was found that all plots are collapsed into the single line. This result suggests that the viscous effect around the chimney plays a role on the appearance of downwash pattern of the hot smoke. It is necessary to check whether the scaling law would work even though the larger scale is imposed, whose Reynolds number based on the chimney scale is large enough and viscous force becomes less important.

Keywords: Smoke plume; Chimney; Cross-flow; Downwash; Turbulence

Introduction

Air pollution, which includes particle dispersion from industrial factories, seriously affects human health and damages the environment [1–6]. Year by year, it is strongly hoped to assess the particle diffusion more precisely for the mitigation of grave air pollution problems, especially for the one released from the chimney as shown in Fig. 1.

Smoke patterns appear randomly one the smoke was issued from the chimney in the cross-wind atmosphere. However, the patterns are mainly categorized into

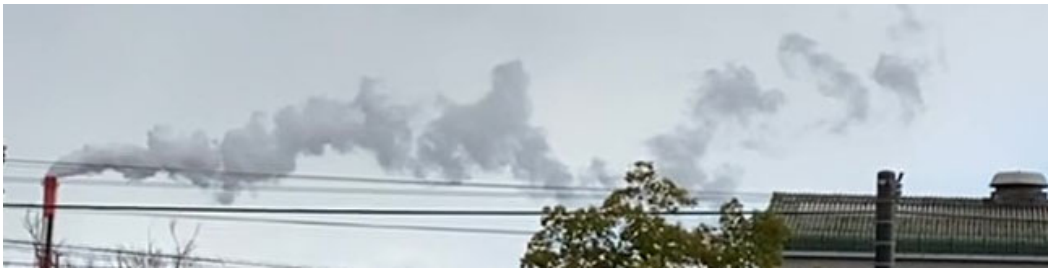

Fig. 1. Example of smoke dispersion from industrial chimney.

Progress in Scale Modeling
AN INTERNATIONAL JOURNAL
https://uknowledge.uky.edu/psmij/

Nomenclature

A_j	Chimney outlet area [m^2]
d_i	Inside diameter of the chimney [mm]
d_o	Outside diameter of the chimney [mm]
E_1	One-dimensional energy spectra (u-spectrum) [m^3/s^2]
E_2	One-dimensional energy spectra (v-spectrum) [m^3/s^2]
F_b	Buoyancy force of smoke [N]
F_{i_j}	Inertia force of smoke [N]
F_{i_w}	Inertia force of wind [N]
F_v	Viscous force [N]
Fr_j	Jet-Froude number [–]
Fr_j^*	Modified jet-Froude number [–]
g	Gravity acceleration [m/s^2]
h	Height of the chimney [mm]
k	Wavenumber [m^{-1}]
L_{UX}	Longitudinal integral scale [mm]
L_{VX}	Lateral integral scale [mm]
M	Mesh size of the grid [mm]
n	Constant number of exponent [–]
Re_d	Reynolds number [–]
Re_M	Mesh Reynolds number [–]
R_L	Turbulence Reynolds number (integral scale) [–]
R_λ	Turbulence Reynolds number (microscale) [–]
T_a	Ambient temperature [K]
U_j	Jet velocity at the top of the chimney exit corrected from U_{j0} [m/s]
U_{j0}	Jet velocity at non-preheated condition from the chimney [m/s]
U_0	Mean velocity of the cross-wind [m/s]
u_{rms}/U_0	Turbulence intensity [%]
x/M	Distance between turbulence generator and measurement point in x-axis [–]
x/d_i	Distance between chimney and measurement point in x-axis [–]
x	Axial direction of cross-wind velocity [mm]
y/d_i	Distance between floor of wind tunnel test section and measurement point in y-axis [–]
y	Axial direction of jet velocity from the chimney [mm]
z	Axial direction of span-wise [mm]

Greek symbols

$\Delta\theta$	Temperature difference between the hot ejected gas (smoke) and the cross-wind (ambient air) [K]
ρ	Density of fluid [kg/m^3]
ρ_a	Density of ambient air [kg/m^3]
ρ_j	Density of preheated jet [kg/m^3]
μ	Viscosity of fluid [kg/m·s]
η	Kolmogorov dissipation scale [mm]
λ	Microscale [mm]
Π	Pi-number [–]

several typical ones based on the characteristic motion of the smoke behind the chimney. Special attention should be paid to the downwash smoke pattern, such that the ejected smoke is "pushed back" downward and smoke is distributed toward the ground behind the chimney. Once this mode appears, the people living in downstream region behind the chimney are directly exposed the harmful gas that may potentially cause severe health damage [7–11]. Therefore, the higher-order prediction of the appearance of downwash patterns ejected from high-rise chimneys in the natural wind is strongly demanded.

To investigate the forementioned smoke motion in a precise yet convenient manner, it is preferred to design the laboratory experiments using a lab-scale, turbulent wind tunnel. Indeed, rich past researches on the smoke dispersion from a chimney were conducted using a wind tunnel [e.g., 7,10–16]. Huang and Hsieh [7] classified the jet structure, and downwash pattern was identified within certain combinations by the momentum ratio between the cross-wind and the jet velocity. Sekishita et al. [11] investigated the patterns of smoke dispersion from a chimney and conditions for its occurrence. Based on a laboratory work, Brusca et al. [12] investigated the interaction of a continuous plume released from a point source with various obstacles. They used digital image analysis to investigate the downwind influence of obstacles of various shapes and distances from a smoke dispersion source in terms of the aerosol concentrations at several points. Said et al. [13] focused on the coherent structures in the near-wake region of a turbulent round-jet ejected perpendicularly from a chimney into a cross flow and discussed its relation with downwash phenomena. Gupta et al. [15] investigated the downwash effect of a rooftop structure (RTS) on plume dispersion. They attempted to provide design guidance to determine stack height required to avoid the downwash effect for an exhaust placed downwind of the RTS. From those previous works, the appearance of downwash pattern was implied to strongly depend on the local flow structure of cross flow interacting with the obstacles (either jet or chimney itself). Most recently, interestingly, it has been figured out that the turbulence field does affect the appearance of downwash patterns [16], suggesting that the precise study on the appearance of the downwash patterns in the actual scale needs the special wind tunnel which can generate the turbulent field of the natural wind. Nevertheless,

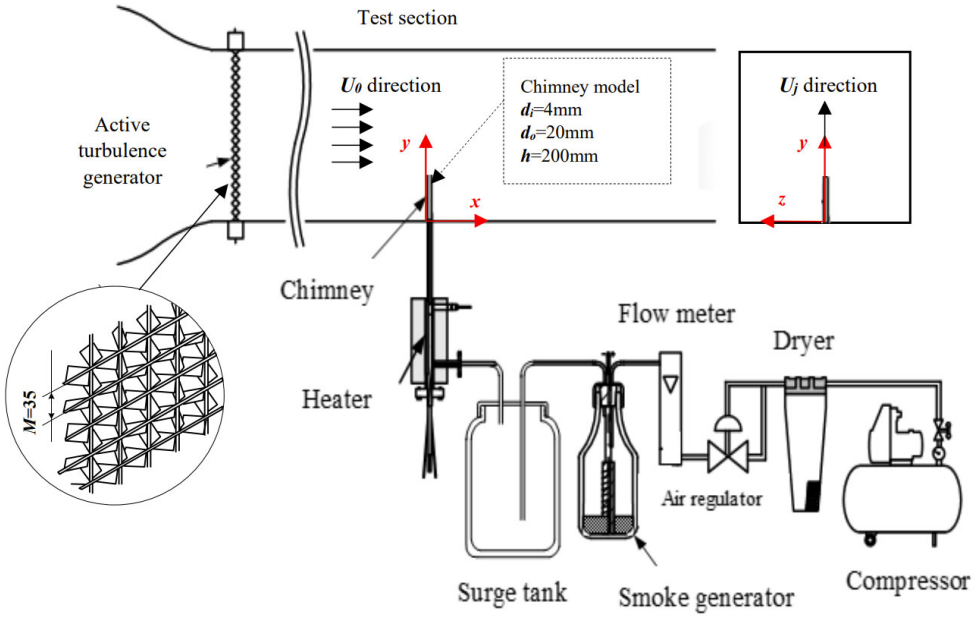

Fig. 2. Wind tunnel, chimney model, and smoke generation system.

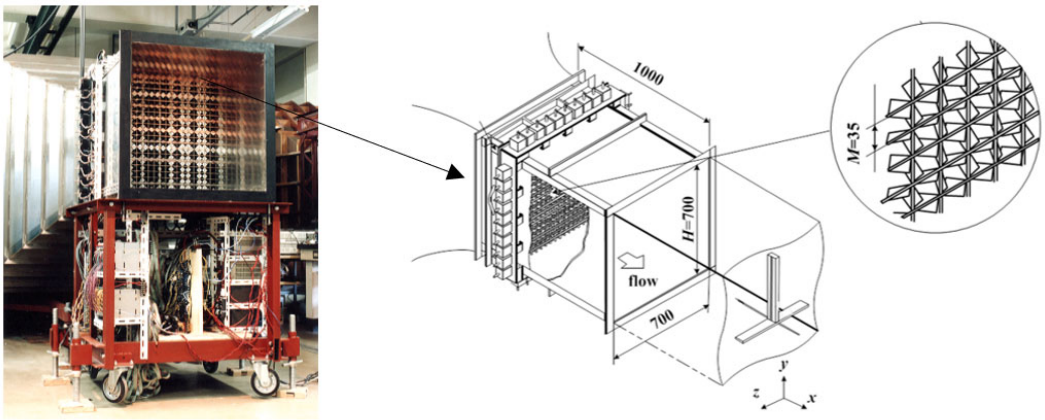

Fig. 3. Active turbulence grid to generate quasi-isotropic turbulence [17].

the boundary of appearance of the downwash pattern is not yet open discussion and yet to be modeled with logical manner. Consequently, this study will introduce the law approach to obtain the scaling law for this problem.

In this study, parametric studies on visualizing the smoke patterns ejected from the chimney are widely made using the specialized wind tunnel, which shall generate quasi-isotropic turbulence field developed by Makita [17]. From the observed results, a law approach is adopted to find the candidate of the scaling law to exhibit the appearance of downwash smoke pattern in a cross-wind. Future work is then addressed based on the discussion of the predicted scaling law in the present study.

Experimental apparatus

Fig. 2 shows the experimental apparatus adopted in this study. The system is identical to our recent work [16]; thus, only brief description is made here. The test section of the adopted wind tunnel consists of 0.7 m in width (z-axis), 0.7 m in height (y-axis), and 6 m in length (x-axis). An active turbulence generator developed by Makita [17] was equipped at the upstream of the test section to produce the quasi-isotropic turbulence, as shown in Fig. 3, with a high turbulence Reynolds number of R_L and R_λ of about 9100 and 390, respectively, at a mean velocity in the cross-wind of U_0 = 5 m/s. It is ensured to generate the large integral scale, large turbulence fluctuations, and the wide inertial

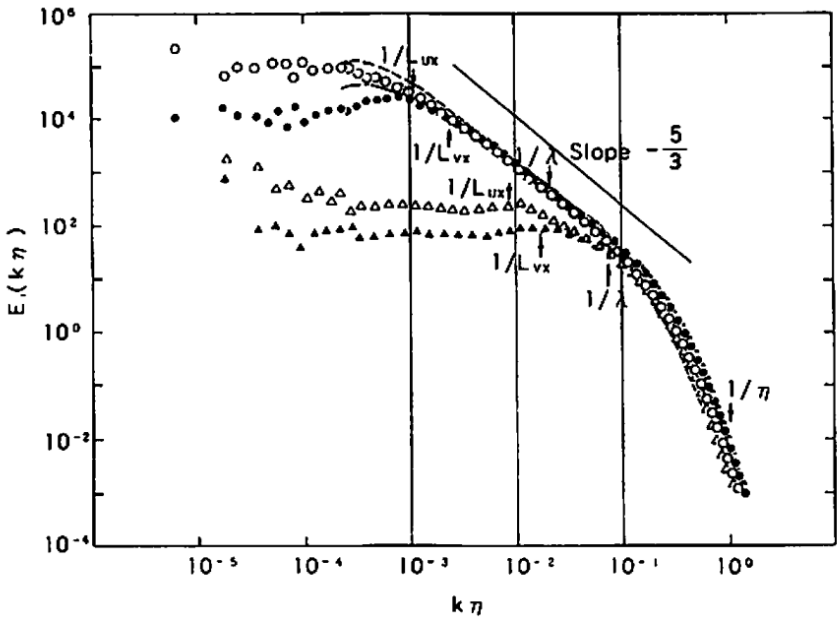

Fig. 4. One-dimensional energy spectra at x/M = 50, E_1 (u-spectrum): (○) quasi-isotropic turbulence, (△) non-quasi-isotropic turbulence, (– – –) grid turbulence, E_2 (v-spectrum): (●) quasi-isotropic turbulence, (▲) non-quasi-isotropic turbulence, (– · – · –) grid turbulence [17].

Table 1. Testing condition.

Temperature difference, $\Delta\theta$ [K]	0, 100, 200
Jet velocity, U_{j0} [m/s], evaluated prior to preheating treatment	0.5, 0.6, 0.8, 1.0, 1.2, 1.4
Cross-wind velocity, U_0 [m/s]	0.3, 0.4, 0.6, 0.8, 1.0

subrange in the energy spectra of velocity fluctuations at 5 m/s of averaged flow speed. The chimney model, with an inside diameter of d_i = 4 mm, outside diameter of d_o = 20 mm, height of h = 200 mm, was placed vertically over the floor of the test section. The smoke was modeled by mist of Shell Ondina Oil 15 and the heated jet was made by an electric heater after the surge tank as shown in the Fig. 2. The center of the chimney on the floor in the test section was the origin of a coordinate system. Here x denotes the cross-wind direction, y denotes the vertical direction parallel to the jet velocity from the chimney, z denotes the spanwise direction. The smoke patterns were visualized by a high-speed camera (Photron FASTCAM SA3, 1000frame/s) and a halogen light.

Fig. 4 shows the energy spectrum of the generated turbulence using the current turbulence generator, which is referred from Ref. 17. The inertial subrange spread for more than two orders of magnitude in wavenumber in the spectrum. These features correspond with those of the grid turbulence with Re_M = 10^6 realized in a large wind tunnel. The active turbulence grid (quasi-isotropic turbulence) generator is homogeneous and quasi-isotropic, with a large turbulence intensity, u_{rms}/U_0, of more than 16% and a large longitudinal integral scale, L_{UX}, of about 200 mm.

The experiments were carried out in the experimental conditions of various temperature differences between the cross-wind and the jet from the chimney, ranging at $\Delta\theta$ = 0–200 K; various jet velocities, which are evaluated at the non-preheated condition (room temperature), ranging at U_{j0} = 0.5–1.4 m/s; and various mean velocities of the cross-wind, ranging at U_0 = 0.3–1.0 m/s, respectively. Although it is not shown here, it has been confirmed that the vertical mean wind velocity profile of the cross flow was uniform around the height of the chimney exit. The applied turbulence intensity in the present study was u_{rms}/U_0 = 9.5%–11.0%. Table 1 summarizes the detailed tested condition applied in this study.

Results and discussion

Two modes of smoke patterns (Mode V and Mode VI)

Two-dimensional (2D) flow visualization experiments are performed using a high-speed camera to distinguish the smoke dispersion patterns from a chimney under certain experimental conditions. A detailed

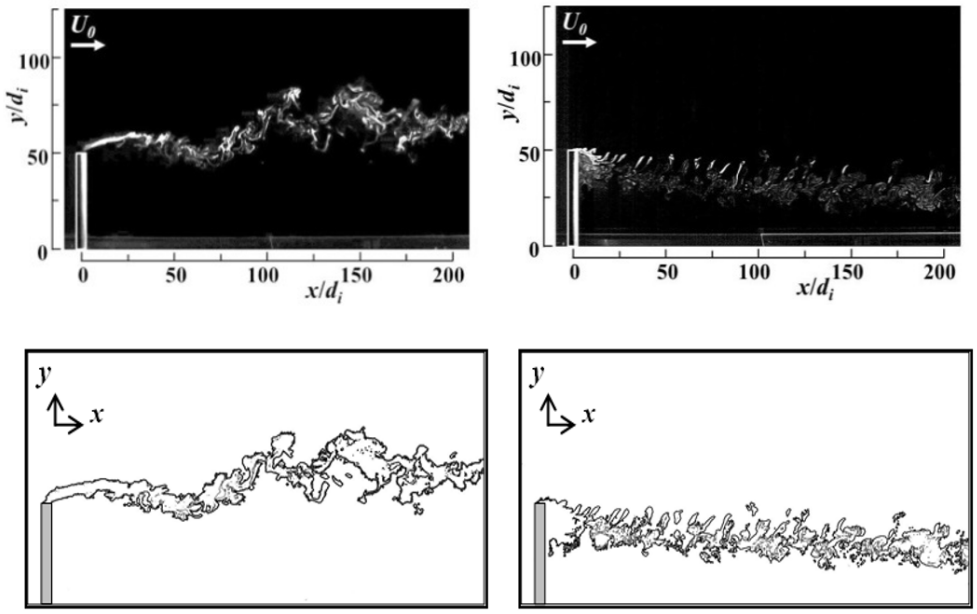

Fig. 5. Representative and distinctive illustration of two patterns of smoke behaviors (Modes V and VI [16]). Left: Mode V, U_0 = 0.6 m/s, U_{j0} = 1.0 m/s, $\Delta\theta$ = 200 K, Right: Mode VI, U_0 = 1.0 m/s, U_{j0} = 0.5 m/s, $\Delta\theta$ = 0 K.

observation of the behaviors of the heated and unheated jets from the chimney in the cross flow is conducted in the quasi-isotropic turbulence case. Fig. 5 shows the typical two types of smoke patterns (i.e., Modes V and VI [16]) obtained by the present experiment. Note that six kinds of the featured patterns are clearly identified in our recent work [16], including bifurcated vortex tubes with and without a strong mutual interaction (Mode I and Mode II), connected hairpin-type vortices (Mode III), the mixture of the coherent and turbulent vortices (Mode IV), the meandering motion (Mode V), and downwash-type structure (Mode VI). Modes I–IV and VI occurred in the grid turbulence case, while Modes V and VI appeared in the quasi-isotropic turbulence case that is studied only in this work. The smoke appeared as the white-colored zone as reflected in the image of the scattered light for visualization purpose.

As clearly shown in the Fig. 5, Mode V exhibits a meandering motion toward downstream, where the smoke is dispersed more widely by the meandering motion due to the large integral scale. Mode VI exhibits downwash, where the smoke is attached behind the top of the chimney and directed to the ground downstream to cause potential health damage by the eddies and the wake behind the chimney. The downwash pattern tends to appear when a high cross-wind velocity was adopted even at heated jet condition. Note that the smoke patterns are categorized by its appearance, so the transient case (fluctuate one mode to the other) cannot be clearly identified (transition is rather continuous). In this study, it is considered that Mode VI is defined as more than half-chance appearance of the "attached smoke behind the chimney". Although the precise definition to categorize the mode is preferred, it is difficult to work further in the present experiment. Currently, numerical simulation is performed to touch more detail on the transition. Therefore, further discussion on any behavior in the transition case is not included in this work. In fact, it was refrained that the main issue on this work is to figure out the key mechanism to identify Modes V and VI (appearance of downwash pattern of the smoke behind the chimney) through scale modeling approach.

Table 2 summarizes the appearance of these modes in tested range of the experimental parameters, such as temperature difference between the cross-wind and the jet from the chimney, $\Delta\theta$, the jet velocity at the non-preheated condition, U_{j0}, and the mean velocity of the cross-wind, U_0. Interestingly, it is noted that the region which appeared as Mode VI clearly depends on the heated smoke temperature in certain experimental conditions, suggesting that the smoke buoyancy would lift-up the smoke to prohibit the occurrence of a downwash pattern. Nevertheless, it is clearly confirmed that the overall trend to appear downwash mode (transition boundary between Mode V and Mode VI) is similar to any preheated cases. This observed fact brings the possibility of having certain scaling law to identify the boundary of two modes, namely, the appearance of the downwash pattern, which is the target of the present study. Please notice that, in Ref. 16 of the previous work, it is interesting to find that the range of the appearance of Mode VI is not sensitive to turbulence. Namely, Mode VI is preferred to appear as a "high-mean flow and low-buoyancy condition" even when using a grid turbulence generator. This suggests that the appearance of downwash pattern (Mode VI) might be insensitive to the

Table 2. Appearance of each mode (Modes V and VI (shaded)) in the quasi-isotropic turbulence with the experimental conditions of $\Delta\theta$, U_{j0}, and U_0.

		Preheated level, $\Delta\theta$ = 0 K						Preheated level, $\Delta\theta$ = 100 K						Preheated level, $\Delta\theta$ = 200 K					
		Jet velocity at non-preheated condition, U_{j0} [m/s]						Jet velocity at non-preheated condition, U_{j0} [m/s]						Jet velocity at non-preheated condition, U_{j0} [m/s]					
		0.5	0.6	0.8	1.0	1.2	1.4	0.5	0.6	0.8	1.0	1.2	1.4	0.5	0.6	0.8	1.0	1.2	1.4
		Jet velocity at the top of the chimney exit, U_j [m/s] (*)						Jet velocity at the top of the chimney exit, U_j [m/s] (*)						Jet velocity at the top of the chimney exit, U_j [m/s] (*)					
		0.5	0.6	0.8	1.0	1.2	1.4	0.5	0.6	0.8	1.0	1.2	1.4	0.5	0.6	0.8	1.0	1.2	1.4
Mean wind velocity, U_0 [m/s]	0.3	VI	V	V	V	V	V	V	V	V	V	V	V	V	V	V	V	V	V
	0.4	VI	VI	V	V	V	V	V	V	V	V	V	V	V	V	V	V	V	V
	0.6	VI	VI	V	V	V	V	VI	V	V	V	V	V	V	V	V	V	V	V
	0.8	VI	VI	VI	V	V	V	VI	VI	V	V	V	V	VI	V	V	V	V	V
	1.0	VI	VI	VI	VI	VI	V	VI	VI	VI	VI	V	V	VI	VI	VI	V	V	V

(*) $U_j = \frac{\rho_a}{\rho_j} U_{j0}$, where ρ_a stands for density of ambient air and ρ_j stands for density of preheated jet

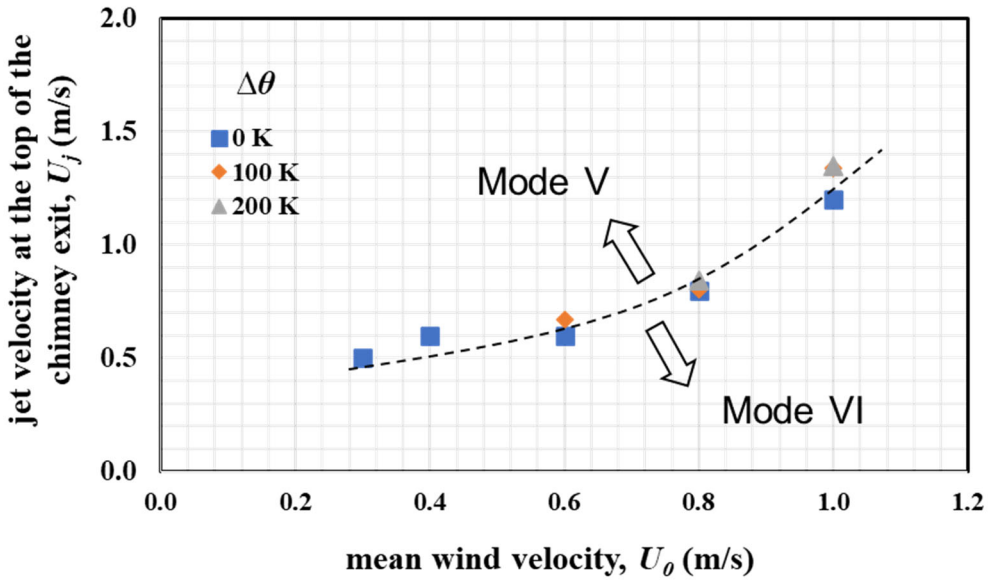

Fig. 6. Summary of the transition boundary to appear as Mode V and Mode VI using U_j and U_0.

turbulence character.

Critical condition for the appearance of downwash pattern (Mode VI)

As presented in Table 2, it is found that transition criteria between two modes in this study are equally affected by the smoke buoyancy (driven by the preheated of the jet), the smoke momentum (i.e., jet velocity at the top of the chimney exit), and the wind momentum (i.e., cross-wind velocity). Fig. 6 replots the boundary of Modes V and VI to show the transition boundary is a clearer manner. The boundary for all conditions studied in the present experiment in the physical plane is summarized. This plane consists of two velocities in the present system, namely, jet velocity at the top of the chimney exit and cross-wind velocity, respectively. It is found that the boundary between Mode V and Mode VI for all preheated conditions studied seems to form a single line, suggesting that the combination of two velocities (U_j and U_0) might be responsible to determine the criteria. In this way, it can be suggested that there is empirical scaling law. However, it is difficult to figure out the physics on this observed fact. Thus, an attempt to introduce the physical consideration to derive the potential scaling law based on law approach [18] would be valuable. The following section tries to obtain the

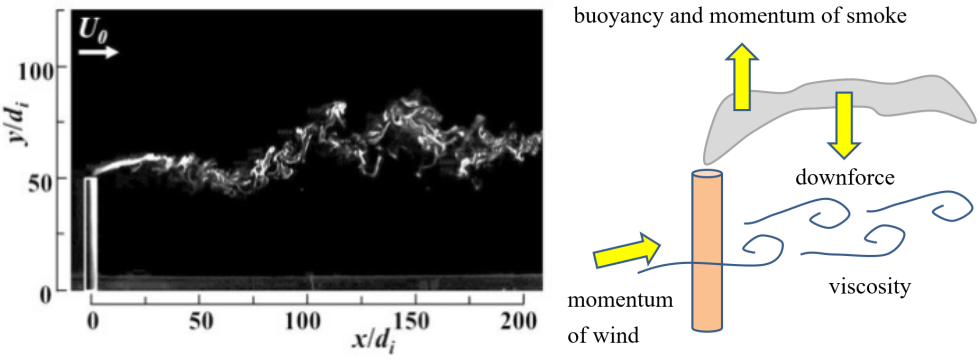

Fig. 7. Potential forces.

scaling law to identify the downwash smoke pattern in the observed range.

Scaling law to provide boundary for the appearance of downwash pattern (Mode VI)

To start to derive the scaling law instructed by Emori's law approach, a potential force to characterize the smoke dynamics shall be considered in the first place. Referred by the observed facts by the experiment, the potential force to characterize the smoke dynamic patterns is depicted as shown in Fig. 7.

Assuming that the observed smoke pattern appeared in a 2D (x-y) plane, there are two directions of force to characterize it. Suppose that there is no backflow against the main flow direction (left to right in this figure). The main force to derive the x-direction of the smoke flow is the wind momentum. On the contrary, the y-direction of the smoke flow is affected by either upward or downward forces. Jet momentum and jet buoyancy are the candidates for the upward force, while the negative pressure induced by the chimney may cause the downward force because the downwash appears immediately behind the chimney. Considering that Reynolds number defined by the mean flow velocity and the outside diameter of the chimney is less than 2300 under the condition considered in this study, a vortex that appeared in the post-chimney zone is one of the candidates as the source of the negative pressure. With this respect, a viscous force induced by the chimney surface would not be immediately eliminated from the candidates of key force to be taken into account to derive the scaling law. Additionally, as described above and the previous work (Ref. 16), the appearance of Mode VI is insensitive to the adopted turbulent condition (the range to the appearance of Mode VI is quite similar irrespective when grid/active turbulence generators were used), suggesting that turbulent characteristics may not be necessary to consider here. Consequently, the following four candidate forces are considered for the law approach.

(1) The smoke buoyancy (driven by the preheated of the jet), F_b

(2) The smoke momentum (i.e., jet velocity at the top of the chimney exit), F_{i_j}

(3) The wind momentum (i.e., cross-wind velocity), F_{i_w}

(4) The viscous force generated by the post-chimney zone, F_v

Note that there are two inertia forces (by the ejected jet, F_{i_j} and cross flow, F_{i_w}), yet they are nearly the same under the condition studied in this work because the imposed jet/flow velocity is within the same range and only a single characteristic length scale (as chimney outside diameter) is considered. Hence, assume that $F_{i\_j} \sim F_{i\_w}$. There are then three independent forces to conform two nondimensional numbers, such as pi-numbers, namely,

$$\Pi_1 = F_b/F_{i\_j} \tag{1}$$

$$\Pi_2 = F_{i\_w}/F_{i\_j} \sim 1 \tag{2}$$

$$\Pi_3 = F_v/F_{i\_j} \sim F_v/F_{i\_w} \tag{3}$$

There is also one additional pi-number to reveal the degree of preheating, Π_4, namely,

$$\Pi_4 = \rho_a/\rho_j \tag{4}$$

where ρ_a stands for density of ambient air and ρ_j stands for density of preheated jet.

It is known that Π_1 is the inverse of Froude number ($= F_{i\_j}/F_b = Fr$) and Π_3 is the inverse of Reynolds number ($= F_{i\_w}/F_v = Re$). Therefore, the jet-Froude number, Fr_j, and the Reynolds number, Re_d, based on the cross-wind velocity, are defined as

$$Re_d = \left(\frac{\rho U_0 d_0}{\mu}\right) \tag{5}$$

$$Fr_j = \left(\frac{U_j^2}{2g\sqrt{A_j/\pi}(T_a/\Delta\theta)}\right)^{1/2} \tag{6}$$

where, U_0 is the mean wind velocity, d_0 is the characteristic length scale (outside diameter of the

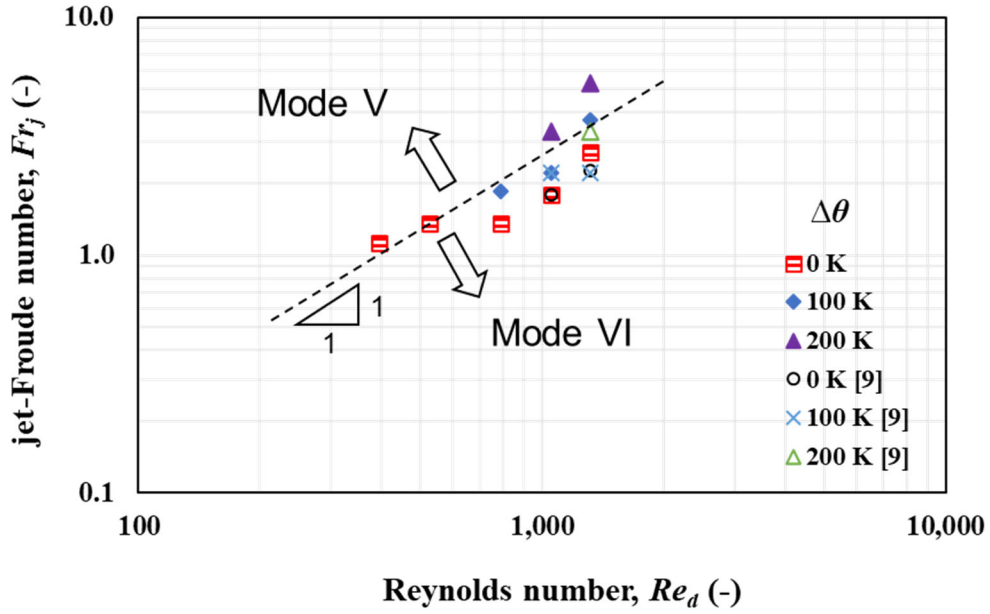

Fig. 8. Jet-Froude number versus Reynolds number of the transition boundary of Modes V and VI. Data from Ref. 9 is also added to support the proposed scaling law.

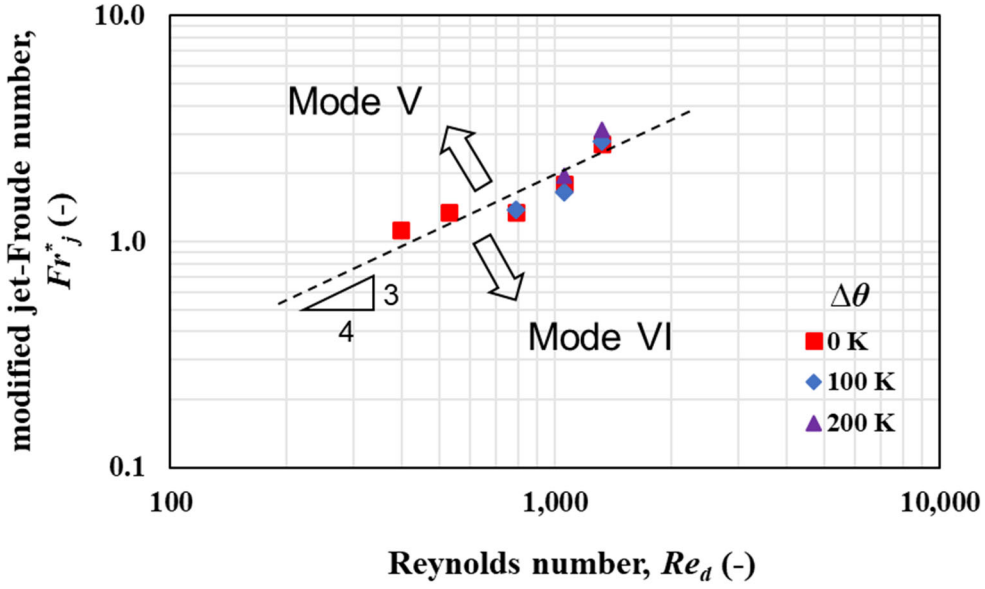

Fig. 9. Modified jet-Froude number versus Reynolds number of the transition boundary of Modes V and VI.

chimney), ρ is the fluid density, μ is the fluid viscosity, U_j is the jet ejecting velocity from the chimney, g is the gravity acceleration, A_j is the chimney outlet area, T_a is the ambient temperature, and $\Delta\theta$ is the temperature difference between hot jet and ambient. Note that the Reynolds number, Re_d, determines the nature of flow around the chimney, defined by the characteristic of cross-wind velocity and the characteristic length of chimney's outside diameter. Also note that the term of nondimensional temperature difference, (T_a/$\Delta\theta$), in Eq. (6), inversed compared with the equation in the reference [9], is applied properly in this work.

In order to check whether these two pi-numbers work to identify the boundary of Modes V and VI observed in the experiment, data plots in Fig. 6 are summarized in Fig. 8 with a logarithm plane. For comparison, reference [9] is also included. According to Ref. 9, smoke downwash shall appear when $Fr^2 \geq 3$, and the jet velocity at the top of the chimney exit is less than or equal to the mean wind velocity ($U_j \leq U_0$). It is shown that the transition boundary between the two modes moderately fits to the single line, suggesting that the

boundary can be summarized by the coupling effect due to the competition of the smoke buoyancy (driven by the preheated of the jet), the smoke momentum (jet velocity at the top of the chimney exit), and the wind momentum (cross-wind velocity). The fitting curve gradient is nearly in unity. Interestingly, the criteria suggested by the past work [9] follow the proposed line as shown above. It is important to note that the suggested criteria by Ref. 9 are only available for preheated conditions since it requires $Fr^2 \geq 3$. In this sense, the present boundary expression is more feasible and universal as compared to the one proposed in the past work [9].

Nevertheless, it is true that data fluctuation for various preheating conditions is not negligible, and further research would be needed. Since one additional pi-number (Π_4) remains, we shall introduce this pi-number for better fit for all conditions. The "modified jet-Froude number" is introduced, defined as

$$Fr_j^* = \Pi_1^{-1} \cdot \Pi_4^n = Fr_j \cdot \left(\rho_a/\rho_j\right)^n \quad (7)$$

Fig. 9 of the modified jet-Froude number is plotted against the wind Reynolds number with the logarithm plane. Note that exponent n in Eq. (7) is adjusted to have best fit curve (currently $n = -1$, by the way).

In this way, it is found that the observed data fit better to the single line, whose exponent is close to 3/4 (= 0.75), suggesting that there are certain physical explanations to satisfy this exponent number (though it is still an open question at present). Additional efforts are necessary to prove the feasibility of the relationship between Fr_j^* and Re_d to bound two modes and go deeper. As noted, the data shows relatively large fluctuation (not organized well), and the covered range is not wide enough. Thus, a numerical approach is preferable, allowing to perform the numerical experiment to identify the universal scaling law in an efficient manner.

Through this work, although it seems that there is concrete scaling law in the present work, it should be concerned whether the proposed scaling law is universal or conditional. For instance, this study only focused in the range of $\Pi_2 \sim 1$ as stated in Eq. (2), and the results are obtained by using the single chimney size (no dependency on the characteristic length is taken into account). Indeed, supposing that the actual scale of the chimney (because the characteristic length of the chimney (its diameter) is in order of meters) is considered, jet Reynolds number becomes extremely larger, suggesting that the viscosity force is relatively negligible. Other forces may be needed to drive the downward force instead of the negative pressure generated by the vortex. To confirm this issue, working on a wide range of testing data is demanded to verify the potential scaling law, which will be also the focus of the future work. As suggested, numerical approach would be valuable on this regard.

Concluding remarks

This study experimentally investigated the smoke behavior ejected from the chimney into the cross-wind, and elucidated the critical condition for the appearance of the downwash pattern. It is found that the wind momentum, the smoke buoyancy, and the smoke momentum are equally responsible for the appearance of the downwash pattern. Such experimental facts were considered to propose the potential scaling law, $Fr_j^* \propto Re_d^{3/4}$, where Fr_j^* stands for the modified jet-Froude number and Re_d stands for Reynolds number defined by characteristic length scale on chimney's outside diameter. Although further verification is needed, this proposed scaling law works well to describe the critical condition of the appearance of the downwash pattern under the condition studied in the present work.

Acknowledgments

This work has been supported by JICA Technical Cooperation Project for ASEAN University Network/Southeast Asia Engineering Education Development Network (JICA Project for AUN/SEED-Net). The first author (XI) would like to express sincere appreciation for their continuous support in conducting this project. Fruitful discussions with Drs. Ju and Matsugi and Profs. Matsuoka and Yamazaki from Toyohashi University of Technology are truly supportive for gaining further understanding on this subject.

References

[1] Aunan, K., Hansen, M. H., Liu, Zh., Wang, Sh., "The hidden hazard of household air pollution in rural China," Environmental Science and Policy 93: 27–33, 2019.

[2] Bayat, R., Ashrafi, Kh., Motlagh, M. Sh., Hassanvand, M. S., Daroudi, R., Fink, G., Kunzli, N., "Health impact and related cost of ambient air pollution in Tehran," Environmental Research 176: 1–12, 2019.

[3] Graber, M., Mohr, S., Baptiste, L., Duloquin, G., Mariet, A. S., Giroud, M., Bejot, Y., "Air pollution and stroke. A new modifiable risk factor is in the air," Revue Neurologique 175(10): 619–624, 2019.

[4] Guo, H., Chang, Zh., Wu, J., Li, W., "Air pollution and lung cancer incidence in China: Who are faced with a greater effect?" Environment International 132: 1–16, 2019.

[5] John, R. B., "Household air pollution from domestic combustion of solid fuels and health," Journal of Allergy Clinical and Immunology, 143: 1979–1987, 2019.

[6] Lee, D., Robertson, Ch., Ramsay, C., Gillespie, C., Napier, G., "Estimating the health impact of air pollution in Scotland, and the resulting benefits of reducing concentrations in city centres," Spatial and Spatio-temporal Epidemiology 29: 85–96, 2019.

[7] Huang, R. F., Hsieh, R. H., "An experimental study of

elevated round jets deflected in a crosswind," Experimental Thermal Fluid Science 27: 77–86, 2002.

[8] Overcamp, T. J., "A review of the conditions leading to downwash in physical modeling experiments," Atmospheric Environment 35: 3503–3508, 2001.

[9] Canepa, E., "An overview about the study of downwash effects on dispersion of airborne pollutants," Environmental Modelling & Software 19: 1077–10887, 2004.

[10] Gnatowska, R., "A study of downwash effects on flow and dispersion processes around buildings in Tandem arrangement," Pol. J. Environ. Stud 24(4): 1571–1571, 2015.

[11] Sekishita, N., Inthavideth, X., Phommachanh, S., "Wind tunnel experiments on smoke structure dispersed from a chimney in a cross flow," Proceeding of the 10th AUN/SEED-NET Regional Conference on Mechanical and Manufacturing Engineering, pp.74–77, 2019.

[12] Brusca, S., Famoso, F., Lanzafameb, R., Garrano, A. M. C., Monforte, P., "Experimental analysis of a plume dispersion around obstacles," Energy Procedia 82: 695–701, 2015.

[13] Said, N. M., Mhiri, H., Palcc, G. L., Bournot, P., "Experimental and numerical analysis of pollutant dispersion from a chimney," Atmospheric Environment 39: 1727–1738, 2005.

[14] Majeski, A. J., Wilson, D. J., Kostiuk, L. W., "Predicting the length of low-momentum jet diffusion flame in cross flow," Combustion Science and Technology 176(12): 2001–2025, 2010.

[15] Gupta, A., Stathopoulos, T., Saathoff, P., "Wind tunnel investigation of the downwash effect of a rooftop structure on plume dispersion," Atmospheric Environment 46: 496–507, 2012.

[16] Inthavideth, X., Nobumasa, S., Phommachanh, S., Nakamura, Y., "Experimental study on the effect of turbulence on hot smoke dispersion ejecting in a cross flow," Journal of Thermal Science and Technology 17(1): 1–14, 2022.

[17] Makita, H., "Realization of a large-scale turbulence field in a small wind tunnel," Fluid Dynamic Research 8: 53–64, 1991.

[18] Saito, K., Williams, F.A., "Scale modeling in the age of high-speed computation," Progress in Scale Modeling, Volume II, Springer, pp.1-18, 2015.